










RESEARCH ARTICLE

Muscle-specific Keap1 deletion enhances force production but does not prevent inactivity-induced muscle atrophy in mice

Edwin R. Miranda^{1,2,3}  | Justin L. Shahtout^{1,4}  | Shinya Watanabe^{1,2}  |
Norah Milam¹ | Takuya Karasawa^{1,2,3}  | Subhasmita Rout^{1,2}  |
Donald L. Atkinson^{1,2}  | William L. Holland^{1,2,3}  |
Micah J. Drummond^{1,2,4}  | Katsuhiko Funai^{1,2,3,4} 

¹Diabetes & Metabolism Research Center, University of Utah, Salt Lake City, Utah, USA

²Department of Nutrition and Integrative Physiology, University of Utah, Salt Lake City, Utah, USA

³Molecular Medicine Program, University of Utah, Salt Lake City, Utah, USA

⁴Department of Physical Therapy & Athletic Training, University of Utah, Salt Lake City, Utah, USA

Correspondence

Katsuhiko Funai, Diabetes & Metabolism Research Center, University of Utah, 15N, 2030E, Salt Lake City, UT 84112, USA.
Email: kfunai@utah.edu

Funding information

HHS | NIH | National Institute on Aging (NIA), Grant/Award Number: AG074535, AG086328, AG079477 and AG076075; HHS | NIH | National Institute of Diabetes and Digestive and Kidney Diseases (NIDDK), Grant/Award Number: DK127979; HHS | NIH | NIDDK | Division of Diabetes, Endocrinology, and Metabolic Diseases (DEM), Grant/Award Number: DK107397, DK112826 and DK130296; HHS | NIH | National Institute of General Medical Sciences (NIGMS), Grant/Award Number: GM144613; HHS | NIH | NHLBI | Division of Intramural Research (DIR), Grant/Award Number: HL170575

Abstract

Immobilization-associated muscle atrophy and weakness appear to be driven in part by oxidative stress. Nuclear Factor Erythroid 2-Related Factor 2 (NRF2) is a critical redox rheostat that regulates oxidative stress responses, and its deletion is known to accelerate muscle atrophy and weakness during aging (sarcopenia) or denervation. Conversely, pharmacologic activation of NRF2 extends mouse lifespan and attenuates sarcopenia. Similarly, deletion of Kelch-like ECH-associated Protein 1 (Keap1), a negative regulator of NRF2, enhances exercise capacity. The purpose of this study was to determine whether muscle-specific Keap1 deletion is sufficient to prevent muscle atrophy and weakness in mice following 7 days of hindlimb unloading (HU). To test this hypothesis, control (Ctrl) and tamoxifen-inducible, muscle-specific Keap1 knockout (mKO) mice were subjected to either normal housing (Sham) or HU for 7 days. Activation of NRF2 in muscle was confirmed by increased mRNA of NRF2 targets thioredoxin 1 (Txn1) and NAD(P)H quinone dehydrogenase 1 (NQO1) in mKO mice. Keap1 deletion had an effect to increase force-generating capacity at baseline. However, muscle masses, cross-sectional area, and ex vivo force were not different between mKO and Ctrl HU mice. In addition, muscle 4-hydroxynonenal-modified proteins and protein carbonyls were unaffected by Keap1 deletion. These data suggest that NRF2 activation improves muscle force production during ambulatory conditions but is not sufficient to prevent muscle atrophy or weakness following 7 days of HU.

KEYWORDS

carbonyl stress, NRF2, oxidative stress, redox, sarcopenia

This is an open access article under the terms of the [Creative Commons Attribution-NonCommercial-NoDerivs](https://creativecommons.org/licenses/by-nc-nd/4.0/) License, which permits use and distribution in any medium, provided the original work is properly cited, the use is non-commercial and no modifications or adaptations are made.

© 2025 The Author(s). *The FASEB Journal* published by Wiley Periodicals LLC on behalf of Federation of American Societies for Experimental Biology.

1 | INTRODUCTION

Maintenance of muscle mass and strength is critical for resiliency during cancer, aging, and immobility.¹ Retention of muscle mass and function is also critical for the preservation of the ability to perform activities of daily living during these processes.² For example, loss of muscle mass and strength in cancer-related cachexia predicts mortality.³ Aging slows the rate of recovery from immobility, and complete recovery is often unattainable, with advanced age leading to progressive loss of muscle mass and function (sarcopenia).⁴ Despite the broad relevance and importance of preserving muscle mass and function, a pharmacologic therapy has yet to be developed to mitigate their losses in these contexts.

Accumulation of reactive oxygen species (ROS) and carbonyl species (RCS) is purported as a major mechanism driving the loss of muscle mass and strength.^{5–10} Specifically, our laboratory and others have recently implicated the accumulation of reactive lipid carbonyls such as 4-hydroxynonenal (4HNE) in driving muscle atrophy and weakness following inactivity models such as hindlimb unloading (HU)¹¹ and denervation.^{7–9} Muscle atrophy and weakness are mitigated by preventing the accumulation of 4HNE-modified proteins with interventions such as overexpression of glutathione peroxidase 4 (GPX4),^{11,12} inhibition of lysophosphatidylcholine acyltransferase 3 (LPCAT3),¹³ and treatment with the RCS scavenger N-acetyl-carnosine¹¹ or liproxstatin.⁹

Nuclear Factor Erythroid 2-Related Factor 2 (NRF2) is a transcription factor that is known to drive the intracellular antioxidant stress response. NRF2 does so by regulating the transcription of genes involved in glutathione synthesis (e.g., glutathione reductase), antioxidant enzymes (e.g., thioredoxin-1), hypoxia response genes (e.g., hemeoxygenase-1), and xenobiotic genes (e.g., NQO1) by binding to Antioxidant Response Element (ARE) promoter regions. Global deletion of NRF2 exacerbates age-related losses in muscle mass, strength, and accelerated frailty.^{14–18} Conversely, treating animals with NRF2 activators such as sulforaphane has been demonstrated to attenuate muscle dysfunction and expand lifespan in male mice.^{19,20} NRF2 activators such as sulforaphane are electrophiles that act on NRF2's negative regulator Kelch-like ECH-associated Protein 1 (Keap1).

Keap1 is an E3 ubiquitin ligase that binds to and ubiquitinates NRF2 to promote its degradation upon reduction of key cysteine residues. Electrophiles such as sulforaphane oxidize these key residues to liberate and stabilize NRF2. Because NRF2 is extensively regulated by posttranslational mechanisms, overexpression of NRF2 is likely not an effective strategy to enhance NRF2 activity.

NRF2 activators are known to have off-target effects, making targeting Keap1 a potentially attractive strategy to enhance NRF2 activity. Recently, muscle-specific inducible Keap1 deletion was shown to activate NRF2 and enhance muscle performance.^{21,22} However, it is unknown if muscle-specific deletion of Keap1 is sufficient to prevent the loss of muscle mass and strength following a bout of inactivity such as hindlimb unloading. The purpose of this study was to test the hypothesis that muscle-specific deletion of Keap1 would prevent disuse-induced oxidative stress, thereby attenuating the loss of muscle mass and strength.

2 | METHODS

2.1 | Animal model

To study the effects of Keap1 deletion in skeletal muscle, we generated a tamoxifen-inducible skeletal muscle-specific knockout (Keap1-mKO, or mKO) mouse. Keap1-mKO mice were generated by crossing conditional Keap1 knockout mice (Keap1^{lox/lox}) acquired from Jackson Laboratory ([RRID:IMSR_JAX:037075](https://www.jacksonlabs.com/strains/037075))²³ with HSA-MerCreMer mice (Figure 1A). Genotypes were determined via PCR using ear punch material as the source of DNA (Figure 1B). For experiments, 8–12-week-old control (Keap1^{lox/lox} without Cre) or Keap1-mKO (Keap1^{lox/lox} with Cre) mice were injected with tamoxifen (7.5 µg/g body mass) for five consecutive days (Figure 1C). After a 2-week washout period from the last day of injection, mice either underwent 7 days of hindlimb unloading (HU) or normal housing (Sham) as previously described¹¹ (Figure 1C). Mice were housed with a 12-h light/dark cycle in a temperature-controlled room. Mice were fasted for 1 h prior to anesthesia via intraperitoneal injection of 80 mg/kg ketamine and 10 mg/kg xylazine and tissue harvest. All experimental procedures were approved by the University of Utah Institutional Animal Care and Use Committee.

2.2 | Hindlimb unloading

A timeline of the experimental design is presented in Figure 1C. Mice underwent 7 days of HU with two mice per cage, as we have previously performed.^{6,11,13} Briefly, mice underwent a modified Morey-Holton hindlimb unloading design²⁴ and were housed 2 per cage with mice of the same sex and genotype. Body weight, water, and food intake were monitored to confirm no excessive weight loss due to malnutrition or dehydration. These mice were checked daily to ensure food and water consumption and to measure body

overnight at 4°C with a concentrated primary antibody targeting myosin heavy chain (MHC) IIa (SC.71, IgG1, 1:100, DSHB), MHC I (BA-D5, IgG2b, DSHB) in 2.5% horse serum in PBS. The next day, sections were incubated for 1 h at room temperature with anti-mouse IgG conjugated to Alexa Fluor 488 (Invitrogen, A28175) (staining MHC IIa), IgG2b conjugated to Alexa Fluor 555 (Invitrogen, A-21147) staining MHC I, and wheat germ agglutinin (Alexa Fluor 647, Invitrogen, W32466). Sections were then washed three times in PBS, fixed with methanol for 5 min at room temperature, and then washed two more times in PBS. Finally, slides were mounted with mounting medium (Vector Laboratories, H-1000). Slides were imaged on a Zeiss Axioscan.Z1 at 20× magnification. Masks for fibers were generated via Cellpose (V3.0)²⁶ and then imported into ImageJ software where CSA was quantified and fluorescent intensity at 488 nm and 555 nm were used to assign fiber type, where 488 nm positive cells were considered MHC IIa fibers, 555 nm positive cells were considered MHC I fibers and fluorescence negative cells were considered MHC IIx or IIb fibers. Type I fibers consist of a negligible proportion in EDL muscles.²⁷

2.5 | Western blotting

Whole muscle lysates were utilized for western blotting. Approximately 20 mg of frozen GAS muscle was cut, weighed, and homogenized in a ground-glass homogenization tube using a mechanical ground glass pestle grinder in 20 volumes of ice-cold RIPA buffer (Thermo Scientific, 89901) supplemented with HALT protease phosphatase inhibitor cocktail with EDTA (Thermo Scientific, 78429). Homogenates were centrifuged for 15 min at 12000×g at 4°C prior to protein estimation of the supernatant via BCA (Thermo Scientific, 23227). Equal protein was then mixed with Laemmli sample buffer with BME to a final protein concentration of 2 mg/mL and denatured by incubating at 95°C for 5 min. Twenty microgram of protein was then loaded onto a 4%–20% gradient TGX gel (Bio-Rad) and separated via electrophoresis (200V, 30 min). Proteins were transferred to nitrocellulose membranes (110V, 1 h) on ice, and then Ponceau stain was placed on the membrane to visualize the membrane-bound protein. Membranes were then blocked in 5% BSA in TBST for 1 h at room temperature with rotation. Membranes were then incubated in primary antibodies targeting 4HNE (1:1000, Abcam, ab48506), p62 (1:1000), or LC3 (1:1000) in 5% BSA in TBST overnight at 4°C with gentle rocking. Membranes were then washed with TBST, incubated in species-appropriate secondaries (1:5000) in 3% milk in TBST for 1 h at room temperature with rotation. After washing the membranes three times with TBST and once with TBS, Membranes were incubated in Western Lightning Plus-ECL (PerkinElmer) and were then imaged

for chemiluminescence (Bio-Rad). Image Lab software was used for densitometric analysis of bands resolved at the predicted molecular weights, and this signal was made relative to the intensity of the Ponceau stain on the membrane.

2.6 | Quantitative reverse transcription polymerase chain reaction

RNA was extracted from approximately 50 mg of TA muscles via a column-based purification kit (Zymo-Research, R2050) according to the manufacturer protocol. Following quantification, 400 ng of RNA was reverse transcribed using an iScript cDNA Synthesis kit (Bio-Rad). Reverse transcription PCR (RT-PCR) was performed with the Viia 7 Real-Time PCR System (Life-Technologies) using SYBR Green reagent (Life-Technologies). Data were normalized to the ribosomal protein L32 gene expression levels and then normalized to the mean of the control sham group. Primer sequences used in this study are as follows: Nqo1 forward: AGAGAGTGCTCGTAGC AGGA, Nqo1 reverse: CAGGATGCCACTCTGAA TCG, Txn1 forward: GCCCTTCTTCCATTCCCTCTG, Txn1 reverse: AGGTGGCATGCATTTGACT, Atf4 forward: CCTGAACAGCGAAGTGTGG, Atf4 reverse: TGGAGAACCCATGAGGTTTCAA, L32 forward: TTCCTGGTCCACAATGTCAA, L32 reverse: GGCTTTTCGGTTCTTAGAGGA.

2.7 | Protein carbonyl assay

Protein carbonyls were assessed via colorimetric assay per the manufacturer's instructions (Cayman Chemical, 10005020). Briefly, 200 µg of GAST protein in 200 µL of RIPA supplemented with protease phosphatase inhibitor cocktail was incubated with 800 µL of dinitrophenylhydrazine (DNPH) in 2.5 M HCl at room temperature for 1 h with constant shaking. DNPH-derivatized protein was then precipitated in trichloroacetic acid and washed with 1:1 ethanol: ethyl acetate to remove unbound DNPH. Pellets were resuspended in Guanidine HCl before being measured for absorbance at 370 nm. Background absorbances derived from the same samples that were treated with 2.5 M HCl without DNPH were subtracted from derivatized samples. Carbonyl content in nmol/mL was calculated by the following equation:

$$\text{Protein Carbonyl (nmol/mL)} = [(CA) / (*0.011 \mu\text{M}^{-1})] (500 \mu\text{L} / 200 \mu\text{L}).$$

An aliquot of the assayed sample was then diluted 1:5 in water and then total protein was measured via BCA. Protein carbonyl content in nmol/mg tissue was then

calculated by dividing the protein carbonyl content in nmol/mL by the protein concentration in mg/mL.

2.8 | Statistics

The data in figures are represented as the means \pm standard error of the mean (SEM). Analyses were performed using GraphPad Prism 9.1.1 software. Figures were made with GraphPad Prism and BioRender. Statistical comparisons were made with two-way analysis of variance (ANOVA) with Bonferroni as post hoc analysis for multiple comparisons where appropriate. Means were statistically significantly different if $p < .05$.

3 | RESULTS

3.1 | Keap1 deletion successfully activates NRF2

Tamoxifen treatment successfully resulted in Keap1 loxP recombination in muscle but not in liver (Figure 1D). Likewise, skeletal muscle Keap1 protein levels were reduced in Keap1-mKO mice compared to control ($p = .0001$, Figure 1E). There was no effect of HU on Keap1 protein abundance in either genotype (Figure 1E). NRF2 target genes thioredoxin 1 (Txn1) ($p < .0001$, Figure 1F) and NAD(P)H quinone dehydrogenase 1 (Nqo1) ($p = .0221$, Figure 1G) were both increased in Keap1 mKO mice compared to control. HU significantly attenuated the increase in Txn1 transcripts in mKO mice ($p = .0235$, Figure 1F) and trended to do the same for Nqo1 transcripts ($p = .0221$, Figure 1G).

3.2 | Effects of muscle-specific Keap1 knockout on body mass, body composition, and muscle mass

As expected, mice that underwent 7 days of HU had significantly lower body mass compared to the sham mice ($p < .0001$, Figure 2A). Keap1-mKO mice weighed significantly lower compared to control mice in the sham condition ($p = .0197$, Figure 2A), though this effect disappeared after HU. The differences in body mass between genotypes were entirely explained by differences in lean mass (Figure 2B). HU reduced muscle masses for almost all hindlimb muscles ($p < .0001$, Figure 2C–G) but genotype had no significant effect on muscle mass with or without HU.

While genotype did not significantly influence muscle masses, Keap1 deletion may have more subtle effects on

myofibers. Muscles from control and Keap1-mKO mice with or without HU were analyzed for fiber type and cross-sectional area (CSA) (Figure 3A). Indeed, Keap1 deletion increased the frequency of fibers with greater CSA for both IIA and IIX/IIB fibers during the sham condition (Figure 3B,C), though this effect disappeared after HU. Additionally, there was a trend for a fiber type switch from IIA to IIX/IIB with Keap1 deletion only with HU (Figure 3D). These effects on CSA distribution (Figure 3F,G) and fiber type proportion (Figure 3H) were not observed in soleus muscle.

3.3 | Keap1 deletion improves skeletal muscle force-generating capacity in ambulatory mice

Hindlimb unloading is known to induce a reduction in force-generating capacity in addition to a loss of skeletal muscle mass.^{6,11} We quantified the force production of soleus and EDL muscles ex vivo and analyzed them as both absolute force (mN) and normalized to muscle area (specific force, mN/mm²). In the sham condition, Keap1 deletion significantly improved absolute and specific force in EDL (Figure 4A,B), but not in soleus (Figure 4C,D). However, the effect of Keap1 deletion on muscle force disappeared in mice that underwent HU.

3.4 | Effect of muscle-specific Keap1 knockout on stress response signaling

To assess muscle carbonyl stress, 4HNE-modified proteins were assessed in gastrocnemius muscles via western blot, and total protein carbonylation was assessed via colorimetric assay. Contrary to our hypothesis, neither HU nor Keap1 influenced levels of 4HNE-modified proteins (Figure 5A,B) or global protein carbonylation (Figure 5C). Given that Keap1 is known to interact with p62, a known regulator of autophagy, we also assessed the abundance of LC3I, LC3II, and p62 in muscles from control and Keap1-mKO mice with or without HU. Both LC3I ($p = .0034$, Figure 5D) and LC3II ($p = .0084$, Figure 5E) were elevated in response to HU with no effect of Keap1 deletion. The LC3II/I ratio was not significantly altered by HU, indicating proportional increases in LC3I and LC3II in response to HU (Figure 5F). Protein abundance of p62 was also unaltered by HU or by Keap1 deletion (Figure 5G). Lastly, we assessed the mRNA of Atf4, an alternative stress response regulator. Similar to other stress indicators we measured, Atf4 mRNA was also not perturbed by HU or Keap1 deletion in muscle (Figure 5H).

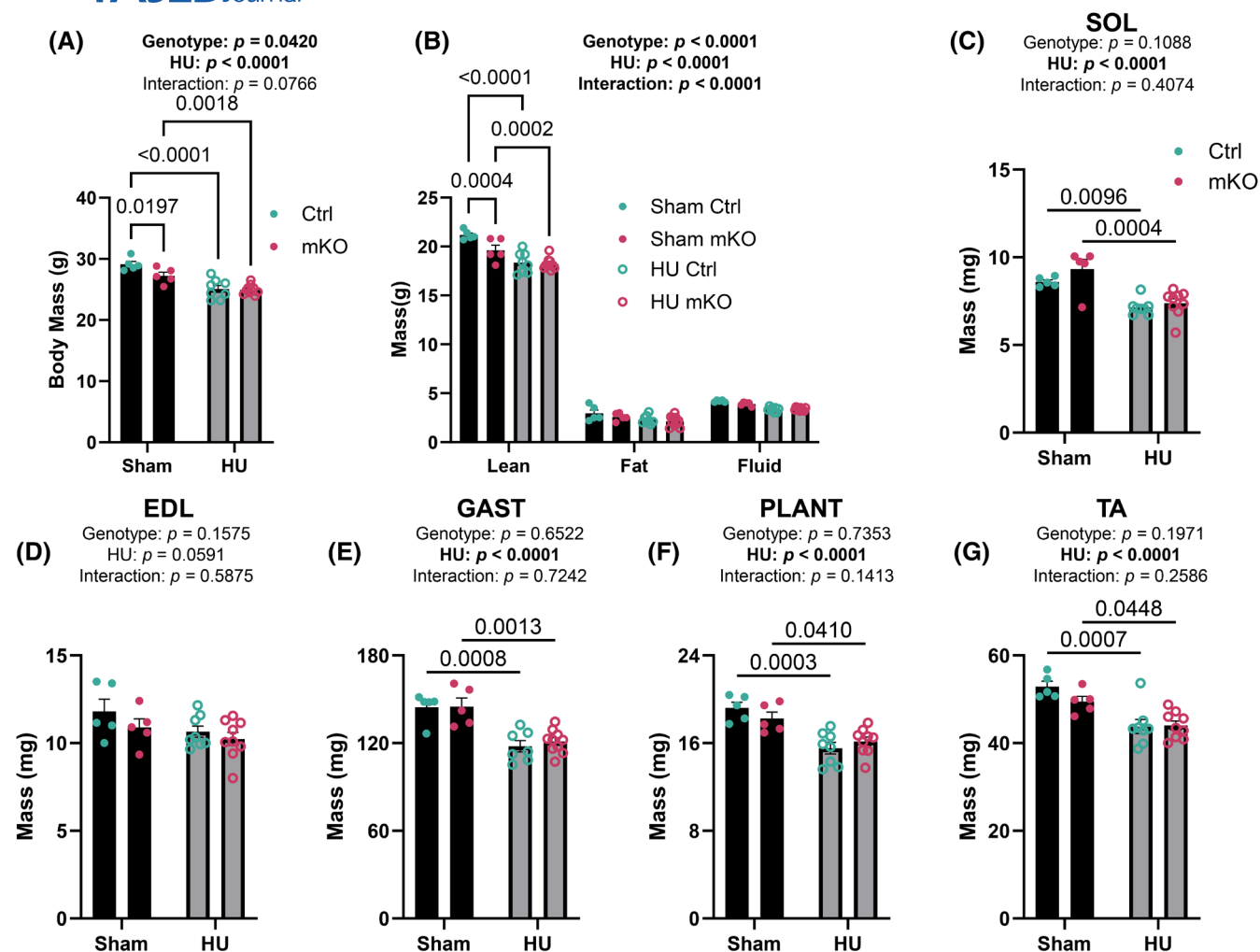


FIGURE 2 Skeletal muscle-specific knockout of Keap1 does not prevent muscle atrophy following 7 days of hindlimb unloading. (A) Post-intervention body mass was lower following HU and in Sham mKO mice. (B) Body composition via NMR reveals lower lean mass in Sham mKO mice and in both Ctrl and mKO mice following HU. (C–G) The average of left and right hindlimb muscle masses taken from mice at the time of dissection was lower following HU but not altered by mKO. Data are Mean \pm SEM and analyzed via two-way ANOVA with Bonferroni post hoc tests. Statistical significance was set to $p < .05$. For all panels, Sham Ctrl $N = 5$, Sham mKO $N = 5$, HU Ctrl $N = 8$, and HU mKO $N = 9$.

4 | DISCUSSION

Maintenance of muscle mass and function during insults that promote their losses is predictive of recovery from injury, disease, and propensity for developing frailty during aging.^{2,4} Lack of the antioxidant transcription factor NRF2 promotes muscle atrophy and weakness similar to that induced by denervation²⁸ and accelerates sarcopenia during aging.^{14–17} Conversely, NRF2 activators and muscle-specific knockout of the NRF2 negative regulator Keap1 enhance exercise capacity²² and extend lifespan in mice.²⁰ However, this is the first study to demonstrate that muscle-specific Keap1 deletion is insufficient to prevent muscle atrophy and weakness following 7 days of HU despite its effect on enhancing force-generating capacity in sham mice.

Muscle-specific deletion of Keap1 significantly increased ex vivo force in EDLs of sham mice. Keap1 deletion had no effect on fiber-type composition, but CSA distribution was slightly shifted toward smaller fibers in the control mice compared to the mKO mice. Nonetheless, this slight shift in CSA size distribution is unlikely to explain the robust differences in force production between control and mKO mice in sham condition. In contrast, there were no differences in the force-generating capacity between control and mKO mice that underwent 7-day HU intervention. This suggests that while Keap1 deletion has the ability to improve muscle force production at baseline, it is insufficient to protect mice from HU-induced muscle weakness.

In contrast, Keap1 deletion had no influence on muscle mass with or without HU. This was despite

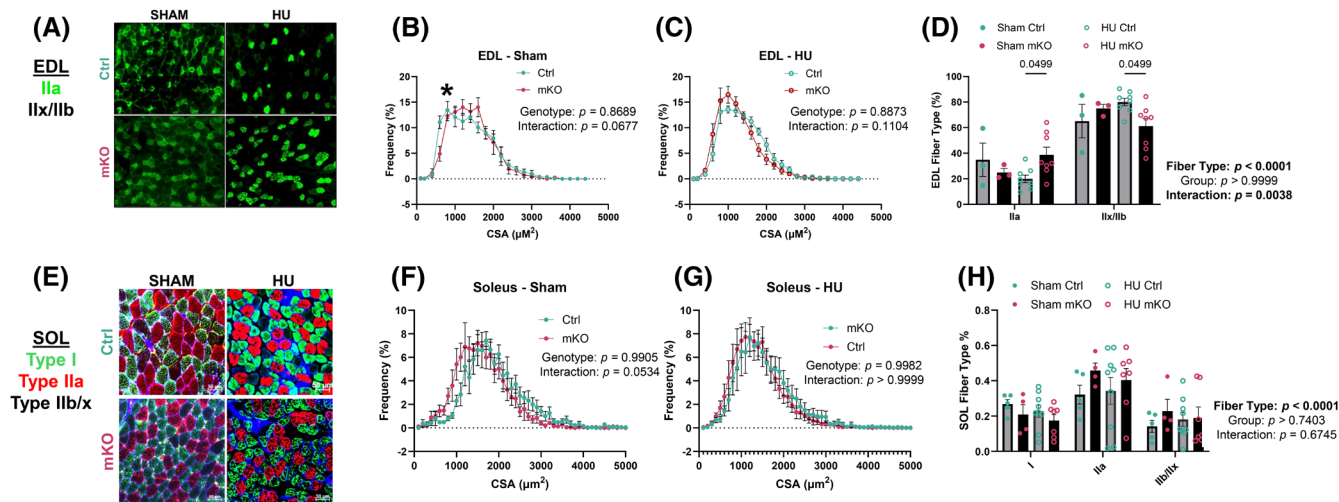


FIGURE 3 Skeletal muscle-specific knockout of Keap1 decreases fast-twitch fiber CSA in EDL but does not alter fiber type in SOL following HU. (A) Representative image of EDL cross section and immunofluorescence targeting Type IIa fibers (green). (B) Frequency of EDL fiber cross-sectional area in Sham and HU (C) was not different between genotypes. (D) Fast, oxidative 2a fibers represent a greater proportion of EDL muscles in HU mKO mice compared to HU Control mice. (E) Representative image of SOL cross section and immunofluorescence targeting Type I (red) and IIa (green) fibers. (F) Frequency of SOL fiber cross-sectional area in Sham and HU (G) was not different between genotypes. (H) Fiber type proportion of SOL muscles in Sham and HU mice was not altered by Keap1 mKO. Data are Mean \pm SEM and analyzed via two-way ANOVA with Bonferroni post hoc tests. Statistical significance was set to $p < .05$. *Indicates post hoc significance. For panels (B–D), Sham Ctrl $N = 3$, Sham mKO $N = 3$, HU Ctrl $N = 7$, and HU mKO $N = 8$. For panels (F–H), Sham Ctrl $N = 4$, Sham mKO $N = 4$, HU Ctrl $N = 9$, and HU mKO $N = 7$.

the previous findings that NRF2 may regulate skeletal muscle mass. Keap1 knockout appeared to successfully upregulate NRF2 activity, evidenced by increased expression of NRF2 target genes *Nqo1* and *Txn1*. Contrary to previous work, including our own,¹¹ neither 4HNE nor total protein carbonyls were elevated with HU. Our laboratory has previously shown that 7 days of HU is sufficient to induce accumulation of 4HNE-modified proteins.¹¹ 4HNE represents only a subset of reactive carbonyls, and 4HNE antibodies likely do not exhibit equal affinity to all 4HNE-conjugated proteins. Thus, it remains possible that HU elevated other RCS not recognized by this antibody. Nevertheless, it is clear that 4HNE conjugation to proteins that are detected by the 4HNE antibodies used in our study (Abcam, ab48506) is not necessary for the loss of muscle mass and function induced by HU in our mice.

Keap1 is chaperoned by p62 to the autophagosome for degradation.²⁹ Therefore, we also tested whether Keap1 deletion altered p62 abundance and autophagic flux. HU resulted in a proportional increase in the abundance of both LC3I and LC3II with no effect from Keap1 deletion. There was also no effect of HU or Keap1 deletion on p62 abundance. Activation of p62 and subsequent Keap1 degradation has been shown to be an important pathway for the activation of NRF2 in response to stress.^{29–31} However, our data suggest that autophagy-mediated Keap1 degradation is neither

involved in skeletal muscle atrophy during HU nor is it altered with Keap1 deletion. We also measured the stress response transcription factor Atf4³² given its ability to heterodimerize with other transcription factors such as NRF2³³ and its potential role in muscle atrophy.³⁴ Similar to other markers of stress we assessed, Atf4 mRNA expression was neither altered by HU nor by Keap1 deletion. Collectively, these data suggest that young mice possess the intrinsic capacity to adequately respond to HU-induced stress to prevent the dramatic accumulation of carbonyl stress and the dramatic activation of stress response pathways.

It is important to note that current studies were performed in young mice and that Keap1 deletion may have protective effects in disuse in old mice that lack sufficient antioxidant capacity.³⁵ For example, our laboratory found that muscle from 20-month-old mice has lower mRNA levels of the NRF2-target gene and anti-ferroptosis gene glutathione peroxidase 4 (GPX4) compared to young mice.¹¹ Muscles from old mice also have attenuated protein abundance of other NRF2-regulated anti-ferroptosis and antioxidant genes such as Glutathione S-transferase Alpha 4, and peroxiredoxins 1 and 2.¹² Alternatively, it is also possible that NRF2 activation in muscle cells is simply ineffective to restore muscle function with immobilization stress such as HU. Similarly, we previously demonstrated that a mouse model overexpressing mitochondria-directed catalase

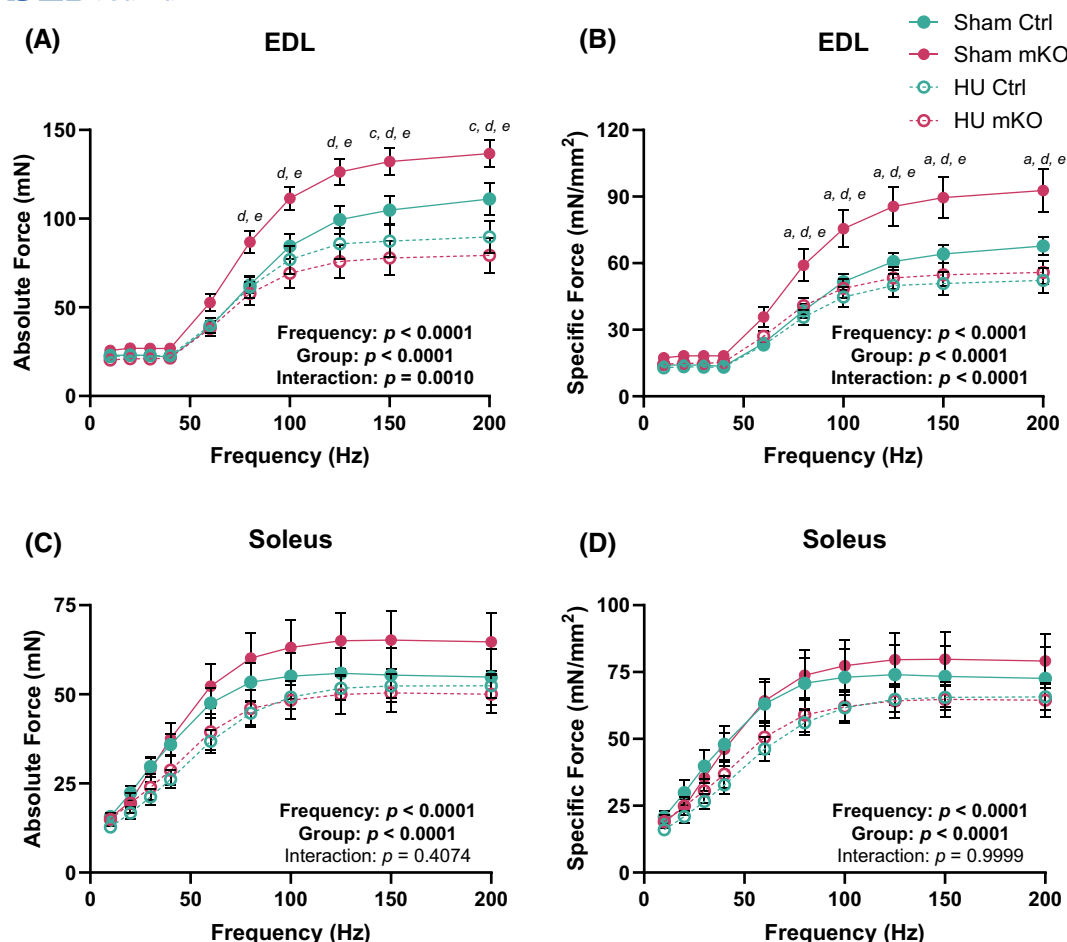


FIGURE 4 Skeletal muscle-specific knockout of Keap1 enhances ex vivo force but does not prevent muscle weakness following 7 days of hindlimb unloading. (A) Force frequency curves quantifying absolute ex vivo force in soleus muscles were higher in Sham mKO mice but were no different between Ctrl and mKO mice following HU. Specific force was calculated by normalizing ex vivo force production to muscle cross-sectional area. (B) Soleus ex vivo specific force was higher in Sham mice but was not affected by Keap1 knockout. Ex vivo absolute (C) and specific force (D) were highest in mKO sham mice. Data are Mean \pm SEM and analyzed via two-way ANOVA with Bonferroni post hoc tests. Statistical significance was set to $p < .05$. Post hoc significance is indicated as follows: *a*—Sham Ctrl versus Sham mKO, *b*—Sham Ctrl versus HU Ctrl, *c*—Sham Ctrl versus HU mKO, *d*—Sham mKO versus HU Ctrl, *e*—Sham mKO versus HU mKO, and *f*—HU Ctrl versus HU mKO. For all panels, Sham Ctrl $N=5$, Sham mKO $N=5$, HU Ctrl $N=8$, and HU mKO $N=9$.

(a gene regulated by NRF2) is insufficient to protect it from HU-induced muscle atrophy.⁶ Paradoxically, deletion of another NRF2 target CuZn-Superoxide Dismutase (SOD1)⁵ and NRF2^{14,16} accelerates sarcopenia. Thus, it is possible that these redox mechanisms of muscle atrophy are more relevant in the context of aging rather than acute immobility. Another possibility is that Keap1/NRF in other cell types abundant in whole muscle tissue, such as endothelial cells, satellite cells, resident macrophages, and fibro-adipogenic precursors (FAPS), is important for muscle mass during immobility.³⁶ Beyond NRF2, Keap1 is known to associate with other proteins such as p62.³⁷ Nonetheless, p62 protein abundance was not affected by Keap1. Finally, chronic activation of NRF2 may induce reductive stress in some contexts, leading to negative outcomes.³⁸ Thus,

it is possible that intermittent activation of NRF2 will demonstrate a more optimal protective stress response.

In conclusion, muscle-specific deletion of Keap1 enhanced EDL ex vivo force production but was not sufficient to prevent atrophy or weakness in mice following 7 days of HU. These findings suggest that chronic activation of NRF2 may not be effective in preventing disuse-induced reduction in skeletal muscle mass and force-generating capacity. It remains possible that targeting the Keap1/NRF2 axis could be protective in other muscle-wasting conditions induced by oxidative stress, particularly for age-associated decline in muscle function. It is also likely that the Keap1/NRF2 axis may play a role in other cell types that reside in the skeletal muscle tissue. Finally, future studies should also consider the possibility that intermittent activation of NRF2 might be a more appropriate

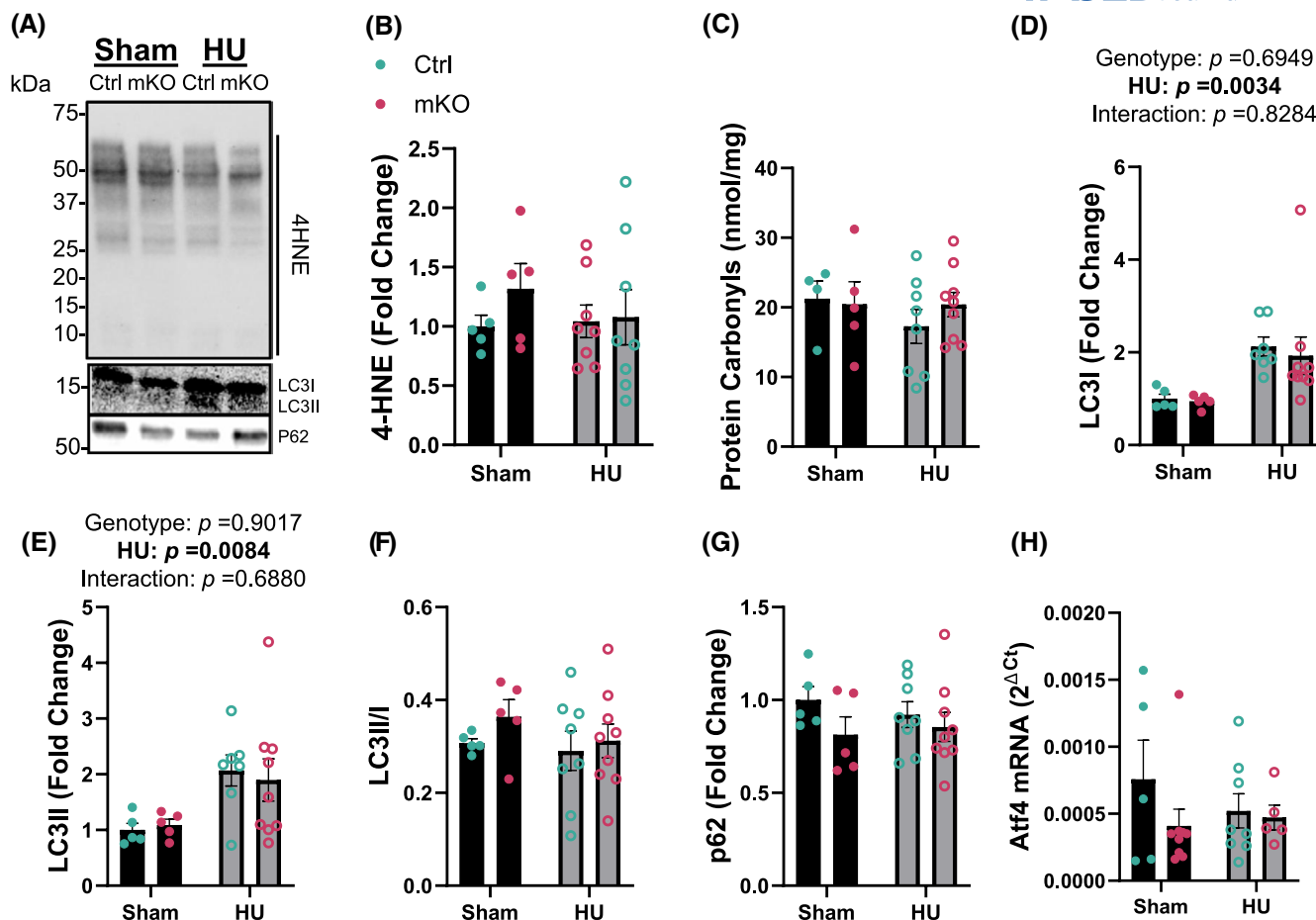


FIGURE 5 Skeletal muscle-specific knockout of Keap1 does not affect autophagic flux or carbonyl stress. (A) Representative western blot for LC3I, LC3II, p62, and 4HNE. (B) Quantification of 4HNE western blots revealed no effect of mKO or 7 days of HU on 4HNE-modified proteins. (C) Global protein carbonylation was also not altered by mKO or 7 days of HU. Both LC3I (D) and LC3II (E) protein abundance was not affected by mKO but was increased following 7 days of HU. However, the proportion of LC3II:LC3I (F) was unaffected by mKO nor 7 days of HU. (G) p62 was also unaffected by mKO and 7 days of HU. (H) The expression of the stress response gene Atf4 was unaltered by mKO or HU. Data are Mean \pm SEM and analyzed via two-way ANOVA with Bonferroni post hoc tests. Statistical significance was set to $p < .05$. For all panels except C, Sham Ctrl $N=5$, Sham mKO $N=5$, HU Ctrl $N=8$, and HU mKO $N=9$. For panel (C), Sham Ctrl $N=4$ due to lack of sample.

approach in controlling the redox state to suppress muscle atrophy and weakness.

AUTHOR CONTRIBUTIONS

Edwin R. Miranda, William L. Holland, Micah J. Drummond, and Katsuhiko Funai designed the research. Edwin R. Miranda, Justin L. Shahtout, Shinya Watanabe, Norah Milam, Takuya Karasawa, Subhasmita Rout, and Donald L. Atkinson conducted experiments. Donald L. Atkinson and William L. Holland provided reagents necessary for experiments. Edwin R. Miranda analyzed the data. Edwin R. Miranda and Katsuhiko Funai wrote the manuscript. All authors reviewed the manuscript.

ACKNOWLEDGMENTS

This work was supported by NIH grants AG074535, DK127979, DK107397, and GM144613 (to K.F.);

AG086328, AG079477, and AG076075 (to M.J.D.); DK112826, DK130296, and HL170575 (to W.L.H.).

DISCLOSURES

The authors have stated explicitly that there are no conflicts of interest in connection with this article.

DATA AVAILABILITY STATEMENT


Raw data, animals, or germ line preservations, and other source materials relevant to this publication will be made available upon reasonable request.

ORCID

Edwin R. Miranda <https://orcid.org/0000-0003-2370-4118>

Justin L. Shahtout <https://orcid.org/0000-0003-4111-4293>

Shinya Watanabe  <https://orcid.org/0000-0003-1369-9001>

Takuya Karasawa  <https://orcid.org/0000-0001-7901-1607>

Subhasmita Rout  <https://orcid.org/0009-0000-8711-8981>

Donald L. Atkinson  <https://orcid.org/0009-0003-7421-890X>

William L. Holland  <https://orcid.org/0000-0001-9950-1435>

Micah J. Drummond  <https://orcid.org/0000-0001-5961-8890>

Katsuhiko Funai  <https://orcid.org/0000-0003-3802-4756>

REFERENCES

- von Haehling S, Anker SD. Cachexia as a major underestimated and unmet medical need: facts and numbers. *J Cachexia Sarcopenia Muscle*. 2010;1:1-5.
- Janssen I, Heymsfield SB, Ross R. Low relative skeletal muscle mass (sarcopenia) in older persons is associated with functional impairment and physical disability. *J Am Geriatr Soc*. 2002;50:889-896.
- Gannavarapu BS, Lau SKM, Carter K, et al. Prevalence and survival impact of pretreatment cancer-associated weight loss: a tool for guiding early palliative care. *J Oncol Pract*. 2018;14:e238-e250.
- Suetta C, Hvid LG, Justesen L, et al. Effects of aging on human skeletal muscle after immobilization and retraining. *J Appl Physiol* (1985). 2009;107(4):1172-1180. doi:10.1152/japplphysiol.00290.2009
- Deepa SS, van Remmen H, Brooks SV, et al. Accelerated sarcopenia in Cu/Zn superoxide dismutase knockout mice. *Free Radic Biol Med*. 2019;132:19-23.
- Eshima H, Siripoksup P, Mahmassani ZS, et al. Neutralizing mitochondrial ROS does not rescue muscle atrophy induced by hindlimb unloading in female mice. *J Appl Physiol*. 2020;129(1):124-132. doi:10.1152/japplphysiol.00456.2019
- Bhattacharya A, Muller FL, Liu Y, et al. Denervation induces cytosolic phospholipase A2-mediated fatty acid hydroperoxide generation by muscle mitochondria. *J Biol Chem*. 2009;284:46-55.
- Bhattacharya A, Hamilton R, Jernigan A, et al. Genetic ablation of 12/15-lipoxygenase but not 5-lipoxygenase protects against denervation-induced muscle atrophy. *Free Rad Biol Med*. 2014;67:30-40.
- Brown JL, Peelor FF III, Georgescu C, et al. Lipid hydroperoxides and oxylipins are mediators of denervation induced muscle atrophy. *Redox Biol*. 2022;57:102518.
- Xu H, Ahn B, Van Remmen H. Impact of aging and oxidative stress on specific components of excitation contraction coupling in regulating force generation. *Sci Adv*. 2022;8:eadd7377.
- Eshima H, Shahtout JL, Siripoksup P, et al. Lipid hydroperoxides promote sarcopenia through carbonyl stress. *eLife*. 2023;12:e85289. doi:10.7554/eLife.85289
- Czyzowska A, Brown J, Xu H, et al. Elevated phospholipid hydroperoxide glutathione peroxidase (GPX4) expression modulates oxylipin formation and inhibits age-related skeletal muscle atrophy and weakness. *Redox Biol*. 2023;64:102761.
- Shahtout JL, Eshima H, Ferrara PJ, et al. Inhibition of the skeletal muscle lands cycle ameliorates weakness induced by physical inactivity. *J Cachexia Sarcopenia Muscle*. 2024;15(1):319-330. doi:10.1002/jcsm.13406
- Miller CJ, Gounder SS, Kannan S, et al. Disruption of Nrf2/ARE signaling impairs antioxidant mechanisms and promotes cell degradation pathways in aged skeletal muscle. *Biochim Biophys Acta*. 2012;1822:1038-1050.
- Huang DD, Fan SD, Chen XY, et al. Nrf2 deficiency exacerbates frailty and sarcopenia by impairing skeletal muscle mitochondrial biogenesis and dynamics in an age-dependent manner. *Exp Gerontol*. 2019;119:61-73.
- Ahn B, Pharaoh G, Premkumar P, et al. Nrf2 deficiency exacerbates age-related contractile dysfunction and loss of skeletal muscle mass. *Redox Biol*. 2018;17:47-58.
- Kitaoka Y, Tamura Y, Takahashi K, Takeda K, Takemasa T, Hatta H. Effects of Nrf2 deficiency on mitochondrial oxidative stress in aged skeletal muscle. *Physiol Rep*. 2019;7:e13998.
- Narasimhan M, Hong J, Atieno N, et al. Nrf2 deficiency promotes apoptosis and impairs PAX7/MyoD expression in aging skeletal muscle cells. *Free Radic Biol Med*. 2014;71:402-414.
- Bose C, Alves I, Singh P, et al. Sulforaphane prevents age-associated cardiac and muscular dysfunction through Nrf2 signaling. *Aging Cell*. 2020;19:e13261.
- Strong R, Miller RA, Antebi A, et al. Longer lifespan in male mice treated with a weakly estrogenic agonist, an antioxidant, an alpha-glucosidase inhibitor or a Nrf2-inducer. *Aging Cell*. 2016;15:872-884.
- Uruno A, Yagishita Y, Katsuoka F, et al. Nrf2-mediated regulation of skeletal muscle glycogen metabolism. *Mol Cell Biol*. 2016;36:1655-1672.
- Onoki T, Izumi Y, Takahashi M, et al. Skeletal muscle-specific Keap1 disruption modulates fatty acid utilization and enhances exercise capacity in female mice. *Redox Biol*. 2021;43:101966.
- Blake DJ, Singh A, Kombairaju P, et al. Deletion of Keap1 in the lung attenuates acute cigarette smoke-induced oxidative stress and inflammation. *Am J Respir Cell Mol Biol*. 2010;42:524-536.
- Ferreira JA, Crissey JM, Brown M. An alternant method to the traditional NASA hindlimb unloading model in mice. *J Vis Exp*. 2011;49:2467.
- Ferrara PJ, Verkerke AR, Maschek JA, et al. Low lysophosphatidylcholine induces skeletal muscle myopathy that is aggravated by high-fat diet feeding. *FASEB J*. 2021;35:e21867.
- Stringer C, Wang T, Michaelos M, Pachitariu M. Cellpose: a generalist algorithm for cellular segmentation. *Nat Methods*. 2021;18:100-106.
- Chleboun GS, Patel TJ, Lieber RL. Skeletal muscle architecture and fiber-type distribution with the multiple bellies of the mouse extensor digitorum longus muscle. *Acta Anat*. 2008;159:147-154.
- Kitaoka Y, Takeda K, Tamura Y, Fujimaki S, Takemasa T, Hatta H. Nrf2 deficiency does not affect denervation-induced alterations in mitochondrial fission and fusion proteins in skeletal muscle. *Physiol Rep*. 2016;4:e13064.
- Ghosh R, Fatahian AN, Rouzbehani OM, et al. Sequestosome 1 (p62) mitigates hypoxia-induced cardiac dysfunction by stabilizing hypoxia-inducible factor 1alpha and nuclear factor erythroid 2-related factor 2. *Cardiovasc Res*. 2024;120:531-547.
- Xu B, He T, Yang H, et al. Activation of the p62-Keap1-Nrf2 pathway protects against oxidative stress and excessive autophagy

- in ovarian granulosa cells to attenuate DEHP-induced ovarian impairment in mice. *Ecotoxicol Environ Saf*. 2023;265:115534.
31. Yamada M, Iwata M, Warabi E, Oishi H, Lira VA, Okutsu M. p62/SQSTM1 and Nrf2 are essential for exercise-mediated enhancement of antioxidant protein expression in oxidative muscle. *FASEB J*. 2019;33:8022-8032.
32. Ebert SM, Rasmussen BB, Judge AR, et al. Biology of activating transcription factor 4 (ATF4) and its role in skeletal muscle atrophy. *J Nutr*. 2022;152:926-938.
33. He CH, Gong P, Hu B, et al. Identification of activating transcription factor 4 (ATF4) as an Nrf2-interacting protein. Implication for heme oxygenase-1 gene regulation. *J Biol Chem*. 2001;276:20858-20865.
34. Ebert SM, Bullard SA, Basisty N, et al. Activating transcription factor 4 (ATF4) promotes skeletal muscle atrophy by forming a heterodimer with the transcriptional regulator C/EBPbeta. *J Biol Chem*. 2020;295:2787-2803.
35. Lawler JM, Song W, Demaree SR. Hindlimb unloading increases oxidative stress and disrupts antioxidant capacity in skeletal muscle. *Free Radic Biol Med*. 2003;35:9-16.
36. Henrot P, Blervaque L, Dupin I, et al. Cellular interplay in skeletal muscle regeneration and wasting: insights from animal models. *J Cachexia Sarcopenia Muscle*. 2023;14:745-757.
37. Kopacz A, Kloska D, Forman HJ, Jozkowicz A, Grochot-Przeczek A. Beyond repression of Nrf2: an update on Keap1. *Free Radic Biol Med*. 2020;157:63-74.
38. Weiss-Sadan T, Ge M, Hayashi M, et al. NRF2 activation induces NADH-reductive stress, providing a metabolic vulnerability in lung cancer. *Cell Metab*. 2023;35:487-503.

How to cite this article: Miranda ER, Shahtout JL, Watanabe S, et al. Muscle-specific Keap1 deletion enhances force production but does not prevent inactivity-induced muscle atrophy in mice. *The FASEB Journal*. 2025;39:e70464. doi:[10.1096/fj.202402810R](https://doi.org/10.1096/fj.202402810R)